Transverse Nuclear Relaxation in Real Ferromagnets

J. Barak, I. Siegelstein,* A. Gabai, and N. Kaplan
The Racah Institute of Physics, The Hebrew University of Jerusalem, Jerusalem, Israel
(Received 19 June 1973)

The existing theoretical model proposed by Hone, Jaccarino, Ngwe, and Pincus (HJNP) to treat spin-spin relaxations in inhomogeneous lines is extended in order to make it applicable to experimental situations often encountered in real ferromagnetic systems. The transverse relaxation of $Eu^{151,153}$ in ferromagnetic EuO and of Co^{59} in ferromagnetic Co metal was studied by the spin-echo technique as function of external magnetic field $H_0 > 4\pi M$ at low temperatures. Nonexponential echo decays were observed in all cases and the relaxation rates were found to be field dependent. The extended HJNP model was successfully applied to account for the observations in EuO, verifying in a *quantitative* manner the important role played by the indirect spin-spin (Suhl-Nakamura) interaction in the relaxation processes of this system. The analysis also yields detailed information concerning the character of the local distribution of the effective fields acting on Eu nuclei in EuO.

I. INTRODUCTION

Measurements of the transverse relaxation rates of Co^{59} in ferromagnetic cobalt metal and Eu^{153} in ferromagnetic EuO, in external magnetic fields $H_0 > 4\pi M$, were recently reported.[1,2] These relaxation rates, deduced in the preliminary reports[1,2] from the tail ends of spin-echo decay curves, were found to be dependent on external magnetic field, as is expected for a relaxation mechanism governed by the Suhl-Nakamura (SN) interaction.[3,4] The observed relaxation rates were much smaller than those calculated for homogeneous spin systems, and the retardation was ascribed to a local distribution of the nuclear Zeeman levels, in accord with a recent theoretical treatment proposed by Hone, Jaccarino, Ngwe, and Pincus[5] (HJNP).

While the functional field dependence of the reported relaxation rates[1,2] appeared to be in reasonable agreement with the original HJNP model, no satisfactory account could be given at the time for the nonexponential character of the spin-echo decay curves. Subsequently, additional discrepancies were observed upon comparing the experimental ratio of the rates for the two Eu isotopes—as deduced from the decay at the tail ends—to the ratio predicted by the HJNP model. In the present paper, an extension of the HJNP model is developed and the extended model is then utilized to treat in a quantitative manner *all* of the experimental observations, for a wide range of external magnetic field and for both Eu^{151} and Eu^{153}.

The paper is organized as follows: A review of the SN interaction, in a manner appropriate for fcc lattice, is presented in Sec. II. Also included in Sec. II is a brief review of the HJNP model and special attention is given to the difference between the roles played by the SN and the dipolar interactions in inhomogeneous spin systems. In Sec. III the theory is developed to adapt the basic HJNP relaxation formula [Eq. (3.12) in Ref. 5] to some real cases often encountered in practice. In Sec. IV, the experimental observations are presented and analyzed with the help of the extended HJNP model, and conclusions are drawn concerning the validity of the model and concerning the nature of the local distribution of the nuclear Zeeman levels in the samples that have been studied.

II. SPIN-SPIN INTERACTIONS

A. Suhl-Nakamura Interaction in fcc Ferromagnets

One can visualize the indirect SN interaction, say between two nuclear spins in a magnetic medium, by considering the following process: A nuclear spin-flip at site 1 creates a virtual magnon through the transverse part of the nucleus-electron interaction. The virtual magnon is then annihilated by another nuclear spin-flip at site 2. The net result would be a mutual spin-flip at sites 1 and 2, i.e., an effective spin-spin interaction. An outline of the formal derivation of the SN interaction for the particular case of EuO is now presented. The electronic spin Hamiltonian is given by

$$\mathcal{H} = \sum_i g\mu_B \vec{S}_i \cdot \vec{H}_i - 2\sum_{i<j} J_{ik} \vec{S}_i \cdot \vec{S}_k \,, \tag{1}$$

where $\vec{H}_i$ includes external magnetic field, demagnetization, and local Lorentz magnetic fields at site i, and to keep $\mathcal{H}$ in a simple form, it is assumed $\vec{H}_i$ also includes the crystalline anisotropy field. This approximation is further justified in Sec. III A. For EuO, which has the fcc structure, only the exchange integrals between nearest neighbors (nn) J_1 and the next-nearest neighbors (nnn) J_2, would be considered.[6] Under equal magnetic field $\vec{H}_a$ in all the sites, we obtain

$$\mathcal{H} = g\mu_B \vec{H}_a \cdot \sum_i \vec{S}_i - 2J_1 \sum_{nn} \vec{S}_i \cdot \vec{S}_j - 2J_2 \sum_{nnn} \vec{S}_i \cdot \vec{S}_j \,. \tag{2}$$

At low temperatures the excitations of the system are given by the spin-wave energies[6]

$$\epsilon_{\vec{k}} = g\mu_B H_a + 2SJ_1 \sum_{\vec{l}_1} (1 - e^{i\vec{k}\cdot\vec{l}_1}) + 2SJ_2 \sum_{\vec{l}_2} (1 - e^{i\vec{k}\cdot\vec{l}_2}) \ . \quad (3)$$

$\vec{l}_1$ denotes the displacement vectors to the z_1 nearest neighbors (12 for fcc) and $\vec{l}_2$ to the z_2 next-nearest neighbors (6 for fcc), in units of lattice constant a_0.

The hyperfine interaction of a nuclear spin $\vec{I}$ with the electronic spin $\vec{S}$ is

$$\mathcal{H}' = A\vec{I}\cdot\vec{S} \ . \quad (4)$$

Following the SN calculations,[3,4] this $\mathcal{H}'$ is taken as perturbation for the electronic system and mixes states with one excited magnon into the ground state. By expanding $\vec{S}$ in terms of spin-wave-creation and annihilation operators, and by taking the second-order correction to the energy of the ground state, the effective Hamiltonian between the nuclear spins is found to be

$$\mathcal{H}'' = -\frac{SA^2}{2} \sum_{i\neq j} \left(\frac{1}{N} \sum_{\vec{k}} \frac{e^{i\vec{k}\cdot\vec{r}_{ij}}}{\epsilon_{\vec{k}}} \right) I_i^- I_j^+ \ , \quad (5)$$

where r_{ij}, the displacement between two spins, is given in a_0 units. For $r_{ij} \gg 1$, the oscillating part excludes terms of large k and we may take the quadratic approximation of small k,

$$\epsilon_k = g\mu_B H_a + 2SJk^2 \ , \quad (6)$$

where $J \equiv J_1 + J_2$. Replacing the sum over k in Eq. (5) by integration

$$\frac{1}{N} \sum_{\vec{k}} \rightarrow \frac{1}{V_c} \int_{\mathrm{BZ}} d^3k \ ,$$

where v_c is the volume of the Brillouin zone, and extending the integration to infinity, we obtain

$$\mathcal{H}^{\mathrm{SN}} = \frac{-A^2}{16\pi Jn} \sum_{i\neq j} \frac{e^{-\kappa r_{ij}}}{r_{ij}} I_j^- I_j^+ \equiv -\frac{1}{2} \sum_{i\neq j} B_{ij} I_i^- I_j^+ \ , \quad (7)$$

where

$$\kappa \equiv (z_1 H_a / H_e)^{1/2} \ , \quad g\mu_B H_e = 2JSz_1 \ ,$$

and $n = 1$, 2, 4, for sc, bcc, and fcc, respectively, is the number of sites in the unit cell.

From Eq. (3), for $J_1 > 3J_2$ and $H_a = 0$, the spin waves have their maximum energy $32J_1S$, at $X[\vec{k} = (2\pi, 0, 0)]$, while the approximated energy (6) has its maximum $10\pi^2 JS$ at $W[\vec{k} = (2\pi, 2\pi, 0)]$. Thus, the quadratic approximation reduces the terms of large k in Eq. (5). For $r \sim 1$, where the oscillations do not suppress large-k contributions and for $J_1 = 0.73K$ and $J_2 = 0.0975K$ as appropriate for EuO,[7] the real B_{ij} are estimated to be about twice the approximated B_{ij} given by Eq. (7). The approximation of integration to infinity which is also justified because of the oscillating terms in Eq. (5), is accurate up to 10%.

We define f_{ij} by

$$f_{ij} = (1/4\pi\alpha)\, e^{-\kappa r_{ij}} / r_{ij} \ , \quad (8)$$

which leads to

$$B_{ij} = (2A^2/Jz_1 n) f_{ij} \ ,$$

where α is a geometrical factor $\alpha = 2/z_1$ for cubic lattices.

It is convenient to characterize a spin-spin interaction by the method of moments.[8] Comparing the operator form of $\mathcal{H}^{\mathrm{SN}}$ and $\mathcal{H}^{\mathrm{dip}}$, the contribution of $\mathcal{H}^{\mathrm{SN}}$ to the second moment is

$$M_2^{\mathrm{SN}} = \tfrac{1}{3} I(I+1) \sum_j B_{ij}^2 \ . \quad (9)$$

This is the square of the rms width of a resonance line in a homogeneous sample. The line is thus "dynamically" broadened by the SN interaction and its Fourier transform gives the shape of the echo-envelope decay in spin-echo experiments.[8] For homogeneous samples, this shape is approximated by a Gaussian[5] with $\sigma = T_2 \simeq \hbar/(M_2^{\mathrm{SN}})^{1/2}$.

B. Inhomogeneous Broadening

The original SN theory[3,4] treated the homogeneous nuclear systems. Real ferromagnets and antiferromagnets have microscopic broadening; strains, impurities, and other imperfections cause the static magnetic field to vary microscopically from site to site. This broadening may prevent a mutual spin flip of two nuclei, owing to energy conservation, if the difference between their Zeeman energies is greater than the strength of the interaction between them. Such spins may be considered "unlike spins" and terms of the kind $I_i^- I_j^+$ should be omitted in the sums of M_2 and higher moments.[8] This results in higher transverse relaxation times of the spins. HJNP[5] developed a model which treats these relaxations quantitatively. They assumed (a) $\hbar\delta \gg [(\frac{1}{3} I(I+1)]^{1/2} B_{nn}$, where B_{nn} is the interaction between nearest neighbors and δ is the characteristic width of the microscopic distribution $g(\omega)$ of the Zeeman energies $[\int g(\omega)\, d\omega = 1]$. (b) There is no correlation between the difference in the Zeeman energies of any two spins and their relative position. This assumption means that for each spin i, the energies of its neighbors in a given jth shell are distributed according to $g(\omega)$. Thus, not all of these neighbors will be able to "spin flip" with the ith spin. The interaction will be effective only with the spins which are in an energy range of B_{ij} from it. These are a fraction c_j of all the spins in the shell, where $c_j = 2g(\omega)B_{ij}/\hbar$. In the simple model of diluted crystals,[8] c is taken as

the average of c_j and $\sum_j \to c\sum_j$ in every sum, changing the moments M_n into M_n^c,[5]

$$M_2^c = cM_2 , \tag{10}$$

$$M_4^c = 5c^2M_2^2 - \left[\frac{2c^2}{N}\sum_{i\neq j\neq k\neq i} B_{ij}^2 B_{jk}B_{ki} - \left(8 - \frac{3}{2I(I+1)} - 5c\right) c\sum_j B_{ij}^4\right]\left(\frac{I(I+1)}{3}\right)^2$$

In the homogeneous sample ($c=1$), $3 < M_4^c/(M_2^c)^2 < 5$ (Ref. 5) and the dynamic line shape is nearly Gaussian, while for $c \ll 1$, $M_4^c/(M_2^c)^2 \gg 1$ and the dynamic line shape is Lorentzian. This predicts an exponential spin-echo decay. Taking the line shape as truncated Lorentzian, its half-width at half-intensity Δ is given by[8]

$$\Delta = \tfrac{1}{6}\pi[3(M_2^c)^3/M_4^c]^{1/2} . \tag{11}$$

In an improved model, HJNP used a better approximation: $\sum_j A_j \to \sum_j c_j A_j$, where A_j is any term in the calculated moments which is summed over lattice sites. With $1/T_2 = \Delta/\hbar$ they found

$$\left(\frac{1}{T_2}\right)_{in}^{SN} = \frac{\sqrt{3}\,\pi\,\bar{c}g(\omega)}{6\hbar^2}\left(\frac{A^2}{Jz_1n}\right)^2 \times\left[\left(\sum_j f_{ij}^3\right)^{3/2}\Big/\left(\sum_j f_{ij}^5\right)^{1/2}\right] \times [\tfrac{1}{3}I(I+1)]^{1/2}/[8 - 3/2I(I+1)]^{1/2} , \tag{12}$$

where $\bar{c}$ is the natural abundance of the observed isotope.

HJNP treated the dipolar interaction in a similar way. $\mathcal{H}^{dip}$ is given by

$$\mathcal{H}^{dip} = \sum_{i<j} d_{ij}(\tfrac{2}{3}I_i^z I_j^z - \tfrac{1}{6}I_i^+ I_j^- - \tfrac{1}{6}I_i^- I_j^+) ,$$
$$d_{ij} = \tfrac{3}{2}\gamma^2\hbar^2\,\frac{1 - 3\cos^2\theta_{ij}}{(r_{ij}a_0)^3} , \tag{13}$$

where γ is the nuclear gyromagnetic ratio and θ_{ij} is the angle between $\vec{r}_{ij}$ and the direction of the magnetization. d_{ij} replaces B_{ij} in the above calculations to give

$$\left(\frac{1}{T_2}\right)_{in}^{dip} = \frac{\sqrt{3}\,\pi\,\bar{c}g(\omega)}{6\hbar^2} \times\left[\left(\sum_j |d_{ij}|^3\right)^{3/2}\Big/\left(\sum_j |d_{ij}|^5\right)^{1/2}\right] \times [\tfrac{1}{3}I(I+1)]^{1/2}/[1.4 - 0.3/I(I+1)]^{1/2} . \tag{14}$$

There is, however, an operator difference between $\mathcal{H}^{SN}$ and $\mathcal{H}^{dip}$. While $\mathcal{H}^{SN}$ consists only of $I_i^+I_j^-$ parts, $\mathcal{H}^{dip}$ includes terms of the $I_i^zI_j^z$ kind, which contribute fraction $\frac{2}{3}$ of the total Hamiltonian to the moments's sums and do not disappear with the microscopic inhomogeneities. Thus the fraction $\frac{4}{9}$, which is the contribution of these terms to the second moment,[8] is not affected by the inhomogeneous broadening, while the other $\frac{5}{9}$ part is reduced by c, where c is the average fraction of the spins which are not "detuned" by this broadening. In order to study the line shape, $\mathcal{H}^{dip}$ in Eq. (13) is replaced by an effective Hamiltonian

$$\mathcal{H}_{eff}^{dip} = \sum_{i<j} d_{ij}[\tfrac{2}{3}I_i^zI_j^z - c(\tfrac{1}{6}I_i^+I_j^- + \tfrac{1}{6}I_i^-I_j^+)] . \tag{15}$$

Following the standard calculations of moments,[8] this Hamiltonian leads to

$$M_2^c(\text{dip}) = \left(\frac{2+c}{3}\right)^2 M_2(\text{dip}) = \tfrac{2}{3}I(I+1)\left(\frac{2+c}{3}\right)^2\sum_j d_{ij}^2 ,$$

$$M_4^c(\text{dip}) = 3[M_2^c(\text{dip})]^2 - \left\{\frac{c}{3N}\left(\frac{4-c}{3}\right)\left(\frac{2+c}{3}\right)^2 \times\sum_{i\neq j\neq k\neq i} d_{ij}^2(d_{jk} - d_{ik})^2 + \frac{1}{5}\left(\frac{2+c}{3}\right)^2 \times\left[8\left(\frac{1+2c}{3}\right) + \frac{3}{2I(I+1)}\left(\frac{8 - 4c + 5c^2}{9}\right)\right] \times\sum_j d_{ij}^4\right\}\left(\frac{I(I+1)}{3}\right)^2 . \tag{16}$$

The line-shape criterion

$$e = M_4^c(\text{dip})/[M_2^c(\text{dip})]^2 ,$$

which is about 2 for cubic dense crystals with $c=1$,[8] stays almost unaltered while going to the limit $c \ll 1$, where $e \approx 3$, and the line shape remains a Gaussian, narrowed by $\frac{4}{9}$.

In reexamining the method of moments for unlike-spin broadening, Walstedt[9] concludes that including unlike-spin terms in the moments's sum is incorrect if it results in $M_4/M_2^2 \gg 3$ and the corresponding Lorentzian line shape is of the order of less than the expected width from like-spin interaction alone. This criterion does not hold in our case where the opposite situation occurs: The contribution of the detuned spins changes the line shape from Lorentzian (the treatment of HJNP for $c \ll 1$) to Gaussian [Eq. (16)].

When $\mathcal{H}^{SN}$ and $\mathcal{H}^{dip}$ are of the same order, both interactions are added and $\mathcal{H}_{eff}^{dip} + c\mathcal{H}^{SN}$ replaces Eq. (15) in the calculations. Under high inhomogeneous broadening, however, the contribution of SN interaction is reduced and the moments are essentially given by Eq. (16). A good example of these calculations is the resonance of F^{19} in antiferromagnetic MnF_2; for pure crystal the second moment is[9]

$$M_2 = \tfrac{1}{3}M_2^{II}(\text{dip}) + \tfrac{1}{3}M_2^{II}(\text{dip-SN}) + M_2^{II}(\text{SN})$$

$$+\tfrac{1}{2}M_2^{II'}(zz)+M_2^{II'}(\pm\pm)\ . \qquad (17)$$

This M_2 sums the contributions of the dipolar interaction, the SN interaction, and a cross term between the two, I denotes the spins of one sublattice, I′ are the spins of the other, and (zz), $(\pm\pm)$ are the contributions of $I_i^z I_j'^z$ and $I_i^+ I_j'^+$ or $I_i^- I_j'^-$, respectively. The rms linewidth $\sqrt{M_2}/(\hbar\gamma)$ is found to be 2.5 Oe,[9] corresponding to a Gaussian relaxation with $T_2 \simeq \hbar/(M_2)^{1/2} = 16$ μsec while the experimental relaxation, measured by Butler *et al.*,[10] is exponential with $T_2 = 29$ μsec. Under high inhomogeneity, the detuning cancels in Eqs. (17) all but the (zz) term and the first term (which is now reduced by $\frac{4}{6}$). This leads to $T_2^{in} \simeq 3T_2$, which is in good agreement with the experimental results.[10]

III. TRANSVERSE RELAXATION INDUCED BY SUHL-NAKAMURA INTERACTION

A. Eu Nuclei in Ferromagnetic EuO

In order to observe SN transverse relaxations, one has to find a system in which this interaction is at least of the order of the dipolar interaction. This is the situation for Co^{59} in ferromagnetic cobalt[1] and Eu nuclei in ferromagnetic EuO.[2] EuO in particular is a suitable material for such a study. It is nearly an ideal Heisenberg ferromagnet below $T_C = 69.5$ K[11,12] and as will be shown immediately, for both Eu^{151} and Eu^{153} in this system, the inequality $\mathcal{H}^{SN} \gg \mathcal{H}^{dip}$ holds. The following parameters are used in the calculations: $A = hf_0/S$, where $S = \frac{7}{2}$ and $f_0 \simeq 141$ MHz is the NMR frequency extrapolated from fields above saturation to zero field (see Sec. IV C); $n = 4$, $\alpha = \frac{1}{6}$, and $z_1 = 12$ for the fcc lattice; $a_0 = 5.15$ Å; $H_e \simeq 408$ kOe; $J \simeq 0.653$ K; $I^{153} = I^{151} = \frac{5}{2}$; $\gamma^{153}/2\pi = 0.4683$ kHz/Oe and $\gamma^{151}/2\pi = 1.049$ kHz/Oe. The natural abundances are $\bar{c}^{153} = 0.5223$ and $\bar{c}^{151} = 0.4777$. Substituting $H_a = 29$ kOe in Eq. (7) and multiplying Eq. (9) by $\bar{c}^{153}$ for Eu^{153} and by $\bar{c}^{151}$ for Eu^{151}, we obtain

$$M_2^{SN}(Eu^{153}) = 4.7\times10^{-45}\ \text{erg}^2\ ,$$

$$M_2^{SN}(Eu^{151}) = 1.1\times10^{-43}\ \text{erg}^2\ .$$

Similar calculations for the dipolar interaction for a magnetization in the [110] direction give

$$M_2^{dip}(Eu^{153}) = 1.6\times10^{-48}\ \text{erg}^2\ ,$$

$$M_2^{dip}(Eu^{151}) = 3.85\times10^{-47}\ \text{erg}^2\ ,$$

$$M_2^{dip}(Eu^{153}\text{-}Eu^{151}) = 3.35\times10^{-48}\ \text{erg}^2\ ,$$

$$M_2^{dip}(Eu^{151}\text{-}Eu^{153}) = 3.66\times10^{-48}\ \text{erg}^2\ ,$$

where $M_2^{dip}(Eu^{153}\text{-}Eu^{151})$ is the part of the Eu^{153} second moment which is contributed by its $I_i^z I_j^z$ interactions with Eu^{151}, and $M_2^{dip}(Eu^{151}\text{-}Eu^{153})$ is similarly defined. Clearly, then, for the EuO system the SN interaction is dominant and only under extremely severe inhomogenous broadening $\mathcal{H}^{dip}$ may have any effect, even upon the fourth moment which is given by[5]

$$M_4(Eu^{153}) \simeq M_4^{SN}(Eu^{153}) + \tfrac{1}{3}M_2^{SN}(Eu^{151})M_2^{dip}(Eu^{153}\text{-}Eu^{151})\ , \qquad (18)$$

where

$$M_4^{SN}(Eu^{153}) \simeq 4[M_2^{SN}(Eu^{153})]^2\ .$$

Another convenient property of EuO, for the purpose of the present study, is the relatively small crystalline anisotropy of this system. As mentioned earlier,[1,2] a new approach was adopted in the present experiment to the study of the SN interaction. By applying a varying external magnetic field $H_0 > 4\pi M$, the *range* of the SN interaction $[1/\kappa$ in Eq. (7)] could be controlled, and the resulting variation in the relaxation rates could be examined experimentally. Since, for EuO, the anisotropy field is much smaller than H_0, a simple linear relation could be assumed to exist between H_0 and H_a of Eqs. (6) and (7) (see further in Sec. IV C).

B. Nonexponential Decay

Before one can proceed in the SN interaction study on the basis of the discussion in Secs. II and III A, attention should be given to some of the nonideal realities encountered in actual ferromagnets. A ferromagnetic sample may be homogeneous only in an external magnetic field $H_0 \geq DM$ and provided it has a shape of a perfect ellipsoid. In all other cases there always exists a macroscopic inhomogeneity originating from different sites in domains and domains walls in unsaturated samples, and from different parts of a particle or different shapes of particles in saturated particles. Since a perfectly shaped elipsoidal sample of EuO is not easy to come by, the effects of a macroscopic line broadening given by $G(\omega)$ on the measurements, must be examined. An obvious consequence of such broadening is that transient NMR methods rather than cw (continuous waves) method must be employed in the study of spin-spin interactions.

In the absence of a microscopic inhomogeneity, however, the difficulty caused by $G(\omega)$ is a trivial one, and a transient study of the spin system at any part of the $G(\omega)$ distribution should yield the same results and can be analyzed in terms of the original SN theory.[3,4] At the other extreme, if the spin system is subjected *only* to microscopic broadening $g(\omega)$, and assuming that the transient study is performed with low enough H_1 (i.e., $\gamma H_1 \ll \delta$), the analysis once again becomes simple and one may apply directly the basic HJNP formula [Eq. (12)], which predicts a single exponential echo decay at any given ω, with a slope $1/T_1$ proportional to $g(\omega)$. Such a situation may be realized, in principle, in antiferromagnets, where macroscopic

broadening, caused in ferromagnets by shape anisotropy, is absent. In actual ferromagnets none of the above extremes is likely to occur, and as a rule the spin system will be subjected both to macroscopic and microscopic inhomogeneities. Packets of spins from different parts of the sample have different center frequencies ω distributed according to $G(\omega)$, the macroscopic line with a characteristic width $D\omega$. Each packet, in turn, is distributed around ω by the microscopic inhomogeneity according to $g(\omega'-\omega)$ with a characteristic width δ. Two experimental situations, which may pertain to such a system, will now be examined in a detailed manner.

First, assume that a spin-echo experiment is performed on the system at a frequency ω_0 with $\gamma H_1 \ll \delta$. If $D\omega > \delta$, the spins which are sampled in the spin-echo experiment belong to many *different* spin packets. The situation is illustrated in Fig. 1(a), in which the contribution from two distinct spin packets, centered at $\omega=\omega_1$ and $\omega=\omega_2$, are detailed. Clearly, $g(\omega_0-\omega_1)\neq g(\omega_0-\omega_2)$ and thus, even though the spins of both groups are resonating at the same frequency ω_0, they will relax at a *different* distinct exponential rates $(1/T_2)_{g(\omega_0-\omega_1)}$ and $(1/T_2)_{g(\omega_0-\omega_2)}$, where $(1/T_2)_{g(\omega_0-\omega)}$ is given by Eq. (12). The decay of the echo is obtained by convoluting the contribution of each packet, $\exp[-t(1/T_2)_{g(\omega_0-\omega)}]$, over all packets in proportion to their $G(\omega)$ and in proportion to $g(\omega_0-\omega)$—the fraction of the spins with frequency ω_0 that each packet contributes to the echo signal. The shape of the echo decay is thus given by

$$A_1(t,\omega_0)\alpha\int_{-\infty}^{\infty}G(\omega)g(\omega_0-\omega)\times\exp\left[-t\left(\frac{1}{T_2}\right)_{g(\omega_0-\omega)}\right]d\omega\ . \tag{19}$$

When $D\omega \gg \delta$, $G(\omega)$ varies very slowly with ω in the range of frequencies where $g(\omega_0-\omega)\neq 0$ and we obtain a simplified decay function, given by

$$A_2(t,\omega_0)\alpha\int_{-\infty}^{\infty}g(\omega_0-\omega)\times\exp\left[-t\left(\frac{1}{T_2}\right)_{g(\omega_0-\omega)}\right]d\omega\ . \tag{20}$$

A second situation to be considered is that in which a spin-echo experiment is performed at some frequency ω_0^0, with $\gamma H_1 \gg \delta$. As can be shown easily, in such case the echo signal is caused by spins from a rather wide frequency band, which can be represented by some distribution function $F(\omega_0)$ with a characteristic width $\Delta\omega \simeq 2\gamma H_1 \gg \delta$ centered around ω_0^0. In order to find the shape of the echo decay when $D\omega > \delta$, we have to integrate over $F(\omega_0)$ and Eq. (19) becomes

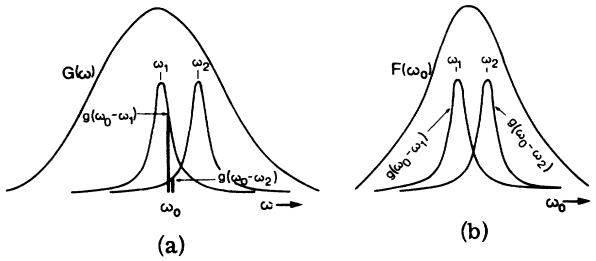

FIG. 1. (a) For macroscopic broadening given by $G(\omega)$, the spins in two packets, distributed according to $g(\omega-\omega_1)$ and $g(\omega-\omega_2)$, have different $g(\omega)$ values at any particular frequency ω_0, which determine their different relaxation rates at that frequency. (b) For a wide distribution $F(\omega_0)$ in the frequencies, which corresponds to high rf field, all the spins in a given packet, such as $g(\omega_0-\omega_1)$ or $g(\omega_0-\omega_2)$, are equally excited. Each spin has different relaxation rates according to its place in the appropriate g distribution.

$$A_3(t)\alpha\int_{-\infty}^{\infty}F(\omega_0)\left\{\int_{-\infty}^{\infty}G(\omega)g(\omega_0-\omega)\times\exp\left[-t\left(\frac{1}{T_2}\right)_{g(\omega_0-\omega)}\right]d\omega\right\}d\omega_0\ . \tag{21}$$

Again, if $D\omega \gg \Delta\omega \gg \delta$, both $G(\omega)$ and $F(\omega_0)$ may be taken out of the integrations, and Eq. (21) is reduced to

$$A_4(t)\alpha\int_{-\infty}^{\infty}g(\omega')\exp\left[-t\left(\frac{1}{T_2}\right)_{g(\omega')}\right]d\omega'\ , \tag{22}$$

where $\omega'=\omega_0-\omega$. This equation has the form of Eq. (20) but has a different meaning. Here the rf pulses equally excite all the spins in a certain packet and every spin contributes to the decay according to its place in the microscopic distribution of frequencies. This situation is illustrated in Fig. 1(b).

An intermediate situation, i.e., $\gamma H_1 \simeq \delta$, was also considered and it was found that in such a case the echo decay will be given again by a relaxation similar to Eq. (20) or (22) provided F and G remain "well-behaved" distributions. Which of the situations so far described is experimentally preferable, depends somewhat on instrumentation, etc. However, for most practical cases, the regime of $\gamma H_1 \gg \delta$ [Fig. 1(b)] is preferable as in this regime the largest fraction of spins will contribute to the echo signal, resulting in an improved signal-to-noise ratio. Another advantage in using $\gamma H_1 \gg \delta$ is that Eq. (22) will then remain valid even if $G(\omega)$ happens to be a noncontinuous distribution—e.g., in a system consisting of a small number of particles—whereas if one studies such a system with $\gamma H_1 < \delta$, Eq. (20) may not be used and the explicit from of G will be required to calculate echo-decay curves by Eq. (19).

IV. EXPERIMENTAL PROCEDURE AND RESULTS

A. Eu Nuclei in EuO

The powder sample of EuO was prepared following a procedure which is a variation of Shafer's method.[13] Europium metal was filed and filtered through a 50-mesh sieve. It was then mixed with Eu_2O_3 in a molar ratio of 2 : 1, pressed into pellets and placed in a tantalum boat in vacuum evaporator. Under pressure of 10^{-5} torr the sample was gradually heated to 1500 °C. After about 10 min, when the vapors of the excess elemental europium ceased to evaporate, the heating was stopped and the sample was allowed to cool in vacuum. The europium was 99.99% pure. The sample was x-ray analyzed and the reflections show an fcc lattice with $a_0 = 5.15$ Å. The quality of the sample was further verified by measuring the Curie temperature. $T_C = 69.5 \pm 0.5$ K was obtained, as expected for pure EuO samples.[12]

The measurements of the decays were carried out, using spin-echo technique, in the frequency ranges of 115–135 MHz for Eu^{153} and 260–295 MHz for Eu^{151}. The rf pulses were produced by commercial high-power pulsed oscillators driven by a Tektronix logic system. In the lower frequencies, the signal was detected by a commercial vacuum-tube television tuner and in higher frequencies by a converter[14] built in our laboratories. The sample was wrapped by a single coil which terminated a coaxial line and was matched by capacitors to the transmitter and to the detector. An external magnetic field up to 60 kOe was achieved by using a superconducting magnet, while for liquid-hydrogen temperatures a Varian magnet with fields up to 31 kOe was used.

In order to deduce the effective anisotropy field H_a acting on the Eu ions from the external field H_0, the macroscopic line shape was also studied. This line is shown for 126 MHz in Fig. 2. The line is nearly Gaussian with derivative extrema separation $DH = 9$ kOe. This is to be compared with $\frac{4}{3}\pi M = 8$ kOe. The symmetry of the line indicates that the particle shapes are distributed randomly and the middle of the line, where the echo decay was measured, corresponds to a demagnetization field of approximately $-2\pi M$. Adding the Lorentz local field $+\frac{4}{3}\pi M$, we find $H_a = H_0 - \frac{2}{3}\pi M \simeq H_0 - 4$ kOe.

The experimental echo decays at different values of H_a are plotted, with a logarithmic amplitude scale in Figs. 3–5. The nonexponential decay in all cases is evident in these plots. In order to determine which of the regimes discussed in Sec. III B is applicable, one has to examine the various widths involved. As an upper limit on δ, one can safely use the cw linewidth of domain-wall nuclei,[7] which yields $\delta < 2\pi \times 80$ kHz. A typical H_1 value,

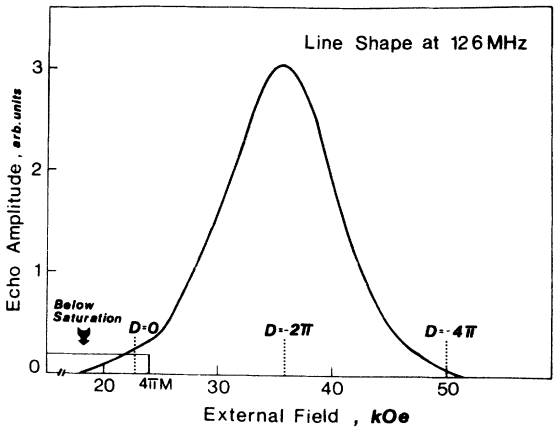

FIG. 2. Macroscopic spin-echo line profile of Eu^{153} in EuO at 126 MHz. The profile is nearly Gaussian with $\sigma = 4.5$ kOe.

at $H_a \simeq 30$ kOe, was $H_1 \simeq 200$ Oe. This is already the enhanced rf field actually seen by the Eu nuclei. For $H_a = 30$ kOe the expected enhancement is $H_{hf}/H_a \simeq 10$, where H_{hf} is the hyperfine field discussed in Sec. IV C. Thus, $H_1 = 200$ Oe corresponds to a direct field of about 20 Oe, produced at the sample coil. Therefore $\Delta\omega = 2\gamma^{153}H_1 \simeq 2\pi \times 200$ kHz. Finally, the macroscopic linewidth, $DH = 9$ kOe, yields $D\omega \simeq 2\pi \times 4.2$ MHz. Thus, $D\omega \gg \Delta\omega \gg \delta$ and Eq. (22) is applicable.

The decay of Eu^{153} at 2.2 K and in $H_a = 29$ kOe is shown in Fig. 4. By best fitting a $g(\omega)$ distribution to this decay using Eq. (22), it is found that a Lorentzian $g(\omega)$ with a width at half-intensity $\delta/2\pi = 3$ kHz (corresponding to a field width of 6.5 Oe) and cut off for $|\omega - \bar{\omega}| > 6\delta$, where $\bar{\omega}$ is the center of $g(\omega)$, is in good agreement with the experimental results. In a remarkable contrast, *no* Gaussian distribution of $g(\omega)$ could be fitted to the experimental data, and as is shown in Fig. 4, even the best fitted Gaussian is far from satisfying. No attempt was made to test additional distribution functions, and therefore one cannot rule out the possibility that some other microscopic distribution function can yield a fit as good as that of the Lorentzian $g(\omega)$ discussed above.

As defined, $g(\omega)$ is the microscopic distribution of the nuclear Zeeman energies. The microscopic distribution in fields $g(H) = \gamma g(\omega)$ is the same for Eu^{151} and Eu^{153}. Therefore, in the frameword of the present model and taking into account the differences in gyromagnetic ratios and natural abundances of the two isotopes, the echo decays of both Eu^{153} and Eu^{151}, for all H_a values, should be calculable without any adjustable parameter except $g(\omega)$. Using a single Lorentzian $g(\omega)$ with $\delta = 2\pi \times 3$ kHz as mentioned above, the echo-decay rates

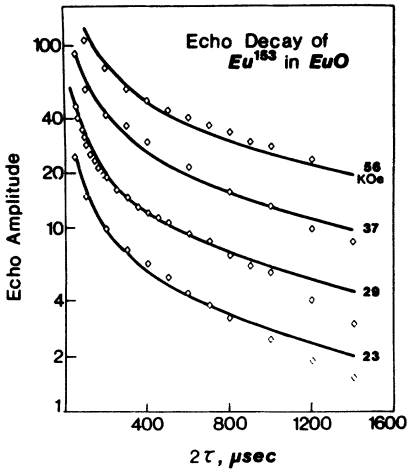

FIG. 3. Echo-decay curves of Eu^{153} in EuO at 4.2 K in different applied magnetic fields. The rhombic points represent the experimental results and the solid curves are the computed, best-fitted decays, derived from the theory of Sec. III.

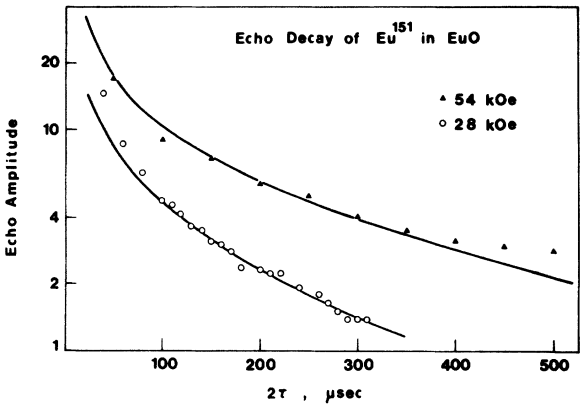

FIG. 5. Echo-decay curves of Eu^{151} in EuO for two field values. The solid curves are the theoretically calculated decays (see Secs. III and IV for details).

for both isotopes and for various H_a values were calculated by Eq. (22) and the calculated results are plotted as solid curves in Figs. 3 and 5. The remarkable agreement between the theoretical predictions and the experimental results, obtained by fitting a single unique $g(\omega)$, seems to confirm the validity of the model discussed in Sec. III B for real ferromagnets.

B. Transverse Relaxation in Metalic Cobalt

The transverse relaxation rates $1/T_2$ for Co^{59} in fcc metallic cobalt were measured at 4.2 K in external magnetic fields $18 < H_a < 60$ kOe.[1] The plot of $1/T_2$ vs H_a is given in Fig. 6. The relaxation rates decrease with increasing external field, indicating the existence of SN interaction between Co^{59} spins. The echo decays are again nonexponential (inset to Fig. 6) and T_2 was deduced from the slopes of the decay tails.

Ferromagnetic fcc cobalt has an effective first-

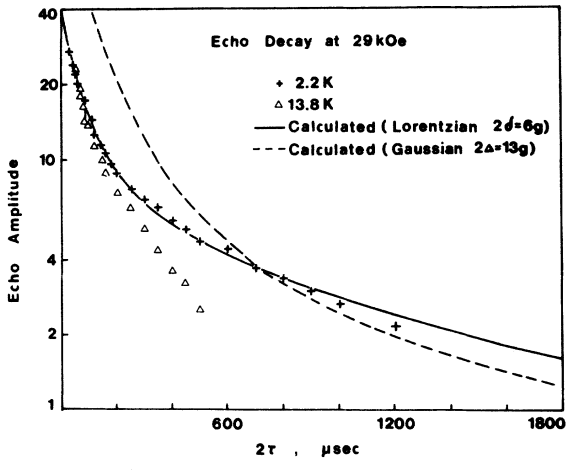

FIG. 4. Echo decay of Eu^{153} in EuO at 29 kOe. The solid line is the "best-fitted" calculated decay for a Lorentzian $g(\omega)$ and the broken line is the best-calculated decay, assuming a Gaussain distribution for $g(\omega)$.

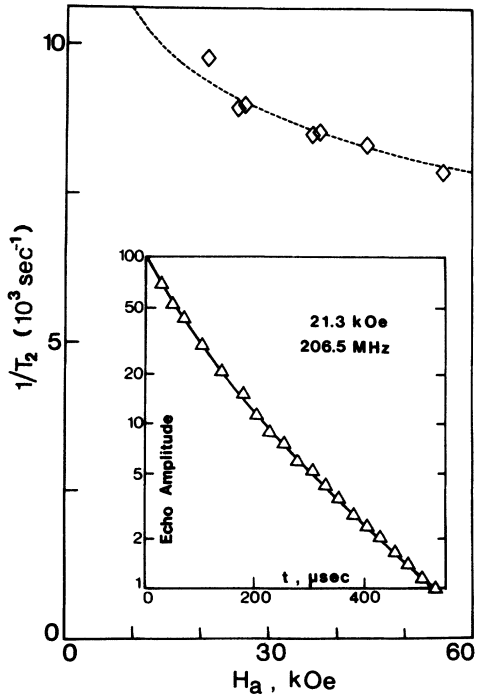

FIG. 6. Experimental transverse relaxation rates of Co^{59} in metallic cobalt in different applied magnetic fields. The inset gives a decay curve for $H_a = 21.3$ kOe.

neighbors exchange interaction with $J \simeq 130$ K, estimated from $T_C \simeq 1400$ K. Using $H_e \simeq 22$ MOe (from $g\beta H_e = 2JSz$), $a = 3.537$ Å, $I = \frac{7}{2}$, $H_a = 30$ kOe, and $\gamma/2\pi = 1.01$ kHz/Oe, we obtain for the homogeneous crystal

$$M_2(\mathrm{SN}) = 7\times10^{-45}\ \mathrm{erg}^2\ ,$$

$$M_2(\mathrm{dip}) = 1.2\times10^{-45}\ \mathrm{erg}^2 \quad \text{for } \vec{M}\,||\langle 110\rangle\ .$$

A cross term M_2(dip-SN) similar to the cross term in Eq. (17) does not exist here, because of the cubic symmetry.

Clearly, $M_2(\mathrm{SN}) > M_2(\mathrm{dip})$ for the homogeneous crystal and $T_2 \simeq \hbar/[M_2(\mathrm{SN}) + M_2(\mathrm{dip})]^{1/2} = 12$ μsec. The observed T_2 is 140 μsec, indicating an inhomogeneous broadening. The contribution to the relaxation rate for $c \ll 1$ of $\mathcal{H}^{\mathrm{dip}}$ alone is $T_2(\mathrm{dip}) = \hbar/[\frac{4}{9}M_2(\mathrm{dip})]^{1/2} = 46$ μsec [see Eq. (16)]. Even this value, which is expected to be an upper limit for T_2, is shorter than the observed one. It is therefore difficult to treat this case quantitatively, by finding the proper $g(\omega)$, as was done with EuO. On the other hand, the following features stand clear: (a) There is a field dependence of T_2; (b) the decay is nonexponential.

C. Discussion

The $g(\omega)$ function for EuO was deduced in Sec. IV A to be a Lorentzian with half-width at half-intensity $\delta/2\pi = 3$ KHz. This value of microscopic broadening has to be consistent with the assumptions of HJNP model. First assumption was that the inhomogeneous broadening is large enough to cause "detuning" of spins. For Eu^{153} the average interaction between nearest neighbors is $[\frac{1}{3}I(I+1)]^{1/2}B_{nn}/h = 2.8$ kHz. This value is of the order of $\delta/2\pi$. For Eu^{151}, B_{nn} is even larger by a factor of $\gamma^{151}/\gamma^{153} = 2.26$. The interaction, however, falls quickly for next-nearest neighbors (by ~50%) and farther neighbors. Thus, it appears that the assumption concerning the magnitude of δ may be relaxed somewhat and it is sufficient that $\hbar\delta \gtrsim [\frac{1}{3}I(I+1)]^{1/2}B_{nn}$. The experimental decay confirms the existence of the inhomogeneous broadening by its shape (non-Gaussian) and by the relaxations which are much longer than $T_2 \simeq \hbar/[M_2^{\mathrm{SN}}(\mathrm{Eu}^{153})]^{1/2} = 15$ μsec—the value for an homogeneous sample.

The second result to discuss is the Lorentzian shape of $g(\omega)$. The inhomogeneous broadening may originate from nonmagnetic impurities such as vacancies, Eu^{3+} ions, Gd atoms, and the like. This will result in a linewidth which is identical to the linewidth of a sample with magnetic ions Eu^{2+} only in the sites of the above impurities. Applying the model of magnetically diluted substances,[8] the inhomogeneous broadening for low concentration of impurities $-c^{\mathrm{imp}} \ll 1$ is Lorentzian, with

$$\delta = 5.3nc^{\mathrm{imp}}\gamma^{153}\mu/a_0^3\ , \tag{23}$$

where n is the number of magnetic ions in a unit cell and $\mu = g\mu_B S$ is their magnetic moment. Substituting in Eq. (23) the value obtained for δ in Sec. IV A, the concentration required, c^{imp}, is found to be 0.059%.

Another source for $g(\omega)$ could be local strains. The change in a_0, that is required to produce the broadening, may be estimated by comparing A^{153} measurements in fcc crystals of BaO, CaO, SrO, and EuO.[7] A linear dependence of A^{153} upon a_0, with a slope $dA^{153}/da_0 = 3.5\times10^3$ Oe/Å. was found,[7] from which one obtains, for $\delta H = 6.5$ Oe:

$$\frac{\delta a_0}{a_0} = \frac{1}{a_0}\left(\frac{dA^{153}}{da_0}\right)^{-1}\frac{\delta H}{S} = 10^{-4}\ . \tag{10}$$

Another value to be discussed is the hyperfine constant A that was used in the calculations. The resonance frequency f versus the field H_0 of the center of the macroscopic line (see Fig. 2) is plotted in Fig. 7. It fits the equation $f = \gamma(H_{hf} - H_a)/2\pi$ where $H_a = H_0 - \frac{2}{3}\pi M$ and $H_{hf} = 303$ kOe. This hyperfine field, corresponding to 140.6 MHz, is to be compared with 138.7 MHz—the zero-field cw frequency found in domain walls,[7] where the external and demagnetization fields are screened. The difference between the two values, 1.9 MHz, could be caused by the local Lorentz field H_L in the domain walls, where one might expect $H_L < \frac{4}{3}\pi M$ because of the variation of the spin direction throughout the wall. The macroscopic variations of H_L may be the origin of the cw linewidth—80 kHz[7]—in a single crystal at zero field.

V. CONCLUDING REMARKS

The model of HJNP, extended to treat real fer-

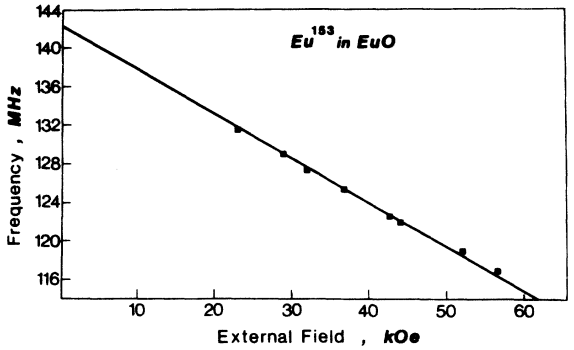

FIG. 7. Plot of the field value needed for maximum Eu^{153} echo amplitude at different transmitter frequencies (see Fig. 2). The slope of the solid line agrees with the Eu^{163} gyromagnetic ratio.

romagnets with combined macroscopic and microscopic broadenings, was shown to provide a satisfactory understanding of the shape of the echo decays for spin system where the SN interaction is dominant. Such a system is the Eu nuclei in EuO. By a single parameter—the inhomogeneous broadening—we were able to calculate the echo decay of both Eu^{151} and Eu^{153} in wide range of external magnetic fields. The dependence of these decays upon external field is shown to provide an effective method to study the SN interaction in ferromagnets, where the line is macroscopically broadened and the anisotropic field is essentially given by the external field.

For spin systems where the dipolar interaction is not negligible compared to the SN interaction, the HJNP model is less applicable. A modification of this model, which takes into account the contributions of $I_i^z I_j^z$ terms of the detuned spins is in good agreement with the experiments of Butler *et al.*,[10] who studied the relaxations rates of F^{19} in antiferromagnetic MnF_2. This model, however, predicts shorter T_2 than observed for Co^{59} in metallic cobalt although it explains the main features of the echo decays.

We have one last remark concerning the temperature dependence of the echo decays, shown in Fig. 4. While very little variations were observed in the decays at liquid-He temperatures, it is seen that the decay becomes much faster at higher temperatures. Neither $\mathcal{H}^{SN}$ nor $\mathcal{H}^{dip}$ are temperature dependent to such an extent, and on the basis of a study of T_1 of EuO as function of temperature,[15] the faster echo decays for $T \gtrsim 5$ K can be ascribed to the influence of spin-lattice processes through the Walstedt mechanism.[16] The effect of this mechanism on the echo decay was calculated to be insignificant below $T \simeq 5$ K, as was indeed verified experimentally. It is not inconceivable, however, that the Walstedt mechanism is responsible for the slight deviations observed at the tail ends of the decays in Fig. 3.

---

*Deceased.

[1] J. Barak and N. Kaplan, Phys. Rev. Lett. **23**, 925 (1969).

[2] J. Barak, I. Siegelstein, A. Gabai, and N. Kaplan, Phys. Rev. Lett. **27**, 817 (1971).

[3] H. Suhl, J. Phys. Radium **20**, 333 (1959).

[4] T. Nakamura, Prog. Theor. Phys. **20**, 547 (1958).

[5] D. Hone, N. Jaccarino, T. Ngwe, and P. Pincus, Phys. Rev. **186**, 291 (1969).

[6] S. H. Charap and E. L. Boyd, Phys. Rev. **133**, A811 (1964).

[7] E. L. Boyd, Phys. Rev. **145**, 174 (1966).

[8] A. Abragam, *The Principles of Nuclear Resonance* (Oxford U. P., London, 1961).

[9] R. E. Walstedt, Phys. Rev. B **5**, 41 (1972).

[10] M. Butler, V. Jaccarino, N. Kaplan, and H. J. Guggenheim, Phys. Rev. B **1**, 3058 (1970).

[11] M. R. Oliver, J. O. Dimmock, A. L. McWhorter, and T. B. Reed, Phys. Rev. B **5**, 1078 (1972).

[12] S. Methfessel and D. C. Mattis, in *Handbuch der Physik*, edited by H. P. J. Wijn (Springer, New York, 1968), Vol. 18, part 1, p. 389.

[13] M. W. Shafer, J. Appl. Phys. **36**, 1145 (1965).

[14] H. Yasuoka, J. Phys. Soc. Jap. **19**, 1182 (1964).

[15] J. Barak and N. Kaplan (unpublished).

[16] R. E. Walstedt, Phys. Rev. Lett. **19**, 146 (1967); Phys. Rev. Lett. **19**, 816 (1967).